PHYSICAL REVIEW B **83**, 041304(R) (2011)

Acoustic and optical phonon scattering in a single In(Ga)As quantum dot

Erik Stock,[1,*] Matthias-Rene Dachner,[2] Till Warming,[1] Andrei Schliwa,[1] Anatol Lochmann,[1] Axel Hoffmann,[1] Aleksandr I. Toropov,[3] Askhat K. Bakarov,[3] Ilya A. Derebezov,[3] Marten Richter,[2,4] Vladimir A. Haisler,[3] Andreas Knorr,[2] and Dieter Bimberg[1]

[1]*Institut für Festkörperphysik, Technische Universität Berlin, Hardenbergstrasse 36, 10623 Berlin, Germany*

[2]*Institut für theoretische Physik, Technische Universität Berlin, Hardenbergstrasse 36, 10623 Berlin, Germany*

[3]*Institute of Semiconductor Physics, Lavrenteva av 13, Novosibirsk 630090, Russia*

[4]*Department of Chemistry, University of California, Irvine, California 92697-2025, USA*

(Received 13 September 2010; published 19 January 2011)

Coupling of acoustic and optical phonons to excitons in single InGaAs/GaAs quantum dots is investigated in detail experimentally and theoretically as a function of temperature. For the theoretical description of the luminescence spectrum, including acoustic and optical phonon scattering, we used the exactly solvable independent boson model. Surprisingly, only GaAs bulk-type longitudinal-optical (LO) phonons are detected in experiment. A quantitatively correct theoretical description of the optical-phonon replica is obtained by including a limited lifetime of the phonons and the dispersion of the LO phonon energy. Similarly, a numerically correct description of the acoustic phonon wings is again based on GaAs bulk material parameters for the phonon dispersion and deformation coupling. In addition, the line shape of the calculated spectra agrees with experiment only when realistic wave functions (e.g., based on eight-band $k\cdot p$ theory) are used for the electron-phonon coupling matrix elements. Gaussian wave functions describing the ground state of a harmonic oscillator fail to describe high-energy tails. Thus, fundamental insights of importance for the correct prediction of properties of nonclassical light sources, based on semiconductor nanostructures, are obtained.

DOI: 10.1103/PhysRevB.83.041304 PACS number(s): 78.67.Hc, 73.63.Kv, 78.67.Lt

Single self-organized semiconductor quantum dots (QDs) (Ref. 1) are most promising for the on-demand generation of single polarized photons as q-bits[2–4] or entangled photon pairs.[5–9] Since QDs can be easily embedded in electrically pumped p-n junctions, compact nanophotonic[10] and nanoelectronic[11] devices can be and have been developed. In contrast to single photon emitters, based on atomic systems,[12] the coupling of a QD to its semiconductor matrix drastically influences the properties of the photons. In particular, the excitonic recombination process is accompanied by a lattice distortion and the generation of polarons.[13,14] This scattering process between the exciton and the phonon leads to a dephasing that results in a reduction of the coherence length of the photons. However, most quantum optic experiments, such as those on indistinguishable photons or quantum cryptography systems using double Mach-Zehnder interferometers,[15] require long coherence length. Also, theory predicts that exciton-phonon scattering may be the limiting factor for generation of entangled photon pairs.[16,17]

On the other hand, luminescence broadening by phonon scattering is useful in experiments on the strong light-matter coupling: The phonon-assisted luminescence can be amplified by the cavity and can be observed even in micropillars containing only a single QD.[18] Hence, to study the strong light-matter coupling theoretically,[19,20] a complete luminescence spectrum, including phonon scattering, must be used.

Phonon scattering has been mostly studied until now on polar CdSe QDs, in which the phonon coupling is much stronger than, for example, in the nonpolar InGaAs QD system. The latter one, however, was most successful for device applications in the past decade, such as for the generation of electrically driven single photons and entangled photon pairs.[3,4,9] Photoluminescence measurements on ensembles of InGaAs QDs lead to the conclusion that coupling to optical phonons might be enhanced in QDs as compared to bulk material.[21] The line shape of a single longitudinal-optical (LO) phonon replica has, however, never been studied experimentally. In this respect, electrically pumped single QDs allow us to study the exciton-phonon interaction on the fundamental level: A single electron-hole pair recombines under generation of a single photon and a phonon.

A number of theoretical approaches exist to describe, at least in part, exciton- and electron-LO phonon interaction. One of them suggested the importance of a second-order elastic interaction between QD charge carriers and LO phonons.[22] The resulting Gaussian shape of the LO replica was, however, found to be an artifact.[23,24] Another strong-coupling model suggested a coupling of LO phonons to excited electronic states in the QD or the wetting layer,[25,26] leading to a more triangular shape of the LO phonon replica. Only recently, an exact solution of the electron-phonon interaction in the quantum optical regime was presented.[27] None of the models has yet been compared with experimental data on single QDs so far.

In this Rapid Communication we report on a comprehensive study of both exciton-acoustic and optical-phonon interaction in a highly efficient single-photon source, based on an electrically driven single InGaAs/GaAs QD. By comparing experimental data with calculated spectra, we demonstrate that phonon coupling strongly depends on a correct and not simplified description of the charge-carrier wave function, phonon dispersion, and the lifetime of the phonons.

Our devices consist of InGaAs/GaAs QDs grown by molecular beam epitaxy with a density of 5×10^8 cm^{-2} embedded in a pin diode structure. Electrical pumping of efficiently only one single QD is achieved by restricting the

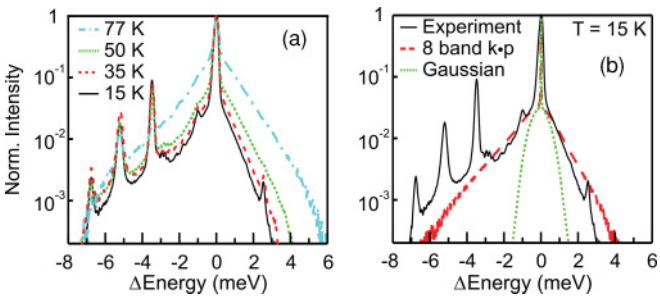

FIG. 1. (Color online) Semilogarithmic plot of the EL intensity of a single QD. (a) With increasing temperature the line broadening increases due to stronger acoustic phonon interaction. (b) Comparison of the measured line shape with two calculated spectra, using alternatively a simple Gaussian (red dashed curve) or a realistic eight-band $k\cdot p$ wave function (green dotted curve).

injection current through an AlO_X aperture. In order to increase the photon out-coupling efficiency, a microcavity consisting of 12 and 3 distributed Bragg mirror layers on the bottom and top of the device, respectively, was grown. The resulting cavity has a center energy at 1.292 eV with a Q factor of 140. A detailed description of our device and single-photon emission at a pump repetition rate of up to 1 GHz can be found in Ref. 28. The electroluminescence (EL) of our device is measured in a microluminescence setup, consisting of a microscope objective [numerical aperture (NA) = 0.8], a triple monochromator with a spectral resolution of 40 μeV, and a liquid-nitrogen-cooled charged couple device detector. In order to obtain spectra with a sufficient large intensity dynamic range, we sum up a series of spectra with 10 s integration time each. The electroluminescence from only one QD can be studied in detail, due to the strong current confinement in our devices.

At a bias of 1.41 V and a current of 5 nA, we sum up a series of 300 spectra of the exciton emission line for each given temperature. In a semilogarithmic plot (Fig. 1), a clear broadening of the emission is visible. The features at −7, −5, and −3.5 meV from the dominating zero phonon line (ZPL) can be attributed to the recombination of other complexes in the QD or to weak luminescence from other QDs. These features vary from device to device and are therefore not related to phonon scattering. These features influence the phonon sidebands and mainly contribute to the difference between theory and experimental data in Fig. 1(b). The temperature dependence of the exciton peak position has been removed from Fig. 1(a) by plotting the spectra on a relative energy scale. In our experiment the linewidth of the ZPL is limited by the spectral resolution of our setup.

At low temperatures (15 and 35 K), the broad sidebands of the ZPL are asymmetric due to spontaneous phonon emission, with larger intensity at the lower-energy side. For increasing temperatures (50 and 77 K) the broadening increases and becomes symmetric. Such properties of the sidebands are typical for acoustic phonon scattering: By emission or absorption of a phonon, the energy of the emitted photon will be reduced or increased, respectively, by the phonon energy. At lower temperatures, the phonon density n_{ph} is low and therefore, due to spontaneous processes, phonon emission [$\sim(n_{\mathrm{ph}}+1)$] of an (acoustic) phonon has a higher probability than the absorption ($\sim n_{\mathrm{ph}}$). Hence, the resulting spectrum is asymmetric. With increasing temperature the phonon density increases ($n_{\mathrm{ph}} \gg 1$) and the probabilities for emission and absorption become equal, resulting in a symmetric spectrum.

For the theoretical description of the luminescence spectrum, including acoustic phonon scattering, we applied the exactly solvable independent boson model:[13,29,30] This model describes the lowest optically active quantum dot transition as a two-level system coupled to phonons by band diagonal interaction. For the numerical evaluation, we used well-known GaAs bulk material parameters for the phonon dispersion and the deformation coupling.[31,32] Therefore, the line shape of the calculated spectra depends only on the electron-phonon coupling matrix elements that are determined essentially by the wave functions of the electrons and holes in the QD. To gain insight into the microscopic interaction and its sensitivity to the character of the electronic wave functions, we compared Gaussian wave functions (i.e., ground state of a harmonic oscillator)[33] and wave functions calculated for a realistic QD using eight-band $k\cdot p$ theory,[34] respectively. Figure 1(b) shows the measured spectrum at 15 K in comparison to the theoretical line shape for both wave-function types. For a Gaussian wave function, often used in theoretical studies, the phonon scattering is strongly underestimated for any energy. In contrast to this, $k\cdot p$ wave functions reproduce the measured spectra very well. The main difference between the two wave-function models is their real space behavior, transferred to the decay of the coupling matrix elements in momentum space: In contrast to Gaussian functions, the more realistic eight-band $k\cdot p$ wave functions allow for an interaction at larger wave numbers. Therefore, larger phonon energies have more impact on the acoustic phonon sidebands. The large difference between the two calculated spectra clearly demonstrates the importance of realistic wave functions already for a qualitatively correct description of electron-phonon scattering. The measured spectra can be reproduced with our model by using realistic eight-band $k\cdot p$ wave functions for temperatures of up to 60 K. Another important result of the modeling of the measured spectra is that they are perfectly reproduced by using GaAs bulk phonon parameters only.

The influence of the wave function is also visible in Fig. 2, where we show the spectral density (containing coupling strength, interaction matrix elements, and phonon dispersion) of the electron-phonon interaction for the two different wave functions. The spectral density at small energies (<10 meV) decays for a Gaussian wave function much faster than for the $k\cdot p$ wave function. This result in energy space can be directly translated to momentum space via the linear dispersion. Even a change of the width of the Gaussian curve never reproduces the measured spectra as well as the eight-band $k\cdot p$ wave function.

Now, in order to study scattering processes of optical phonons experimentally, we sum up a series of 1450 spectra of the LO-phonon replica, resulting in a five times longer integration time than for the acoustic phonon. Figure 3(a) compares two spectra of the same QD under the same bias condition: The black dotted curve shows the exciton emission line around 1.3035 eV. For the second spectrum, the energy scale [on the top of Fig. 3(a)] is shifted by 36.5 meV compared to the bottom scale. Three pronounced peaks are visible in this

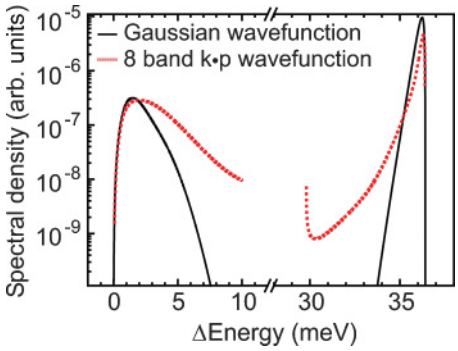

FIG. 2. (Color online) Comparison of the spectral phonon density for two different wave functions. For acoustic phonons (energy <10 meV) the Gaussian wave function (black curves) decreases too quickly, leading to an underestimation of the phonon scattering.

spectrum, and each of them has a "counterpart" in the black spectrum. For other QDs, we also found for almost every intense luminescence line a "counterpart" separated by around −36 meV.

We attribute these corresponding lines to the recombination of an exciton accompanied by the emission of an LO phonon. For different QDs, the phonon energy varies between −35.7 and −36.6 meV with no systematic trend, as compared to the ZPL energy. These energies are comparable to the LO phonon energy of strain-free GaAs bulk material of 36.59 meV.[31] The variation of the phonon energy can be explained by differences in the strain of the GaAs material induced by size and composition of the actual QD.[35] At the energy of the InAs LO phonon replica (30.3 meV), within our intensity dynamic of five orders of magnitude, no luminescence is observed. This is in agreement with the results for acoustic phonon scattering. Consequently, the electron and holes in the QDs interact predominantly with phonons from the surrounding GaAs. The InAs phonon interaction is at least one order of magnitude less. No emission caused by localized InAs-type phonons in the QD is observed.

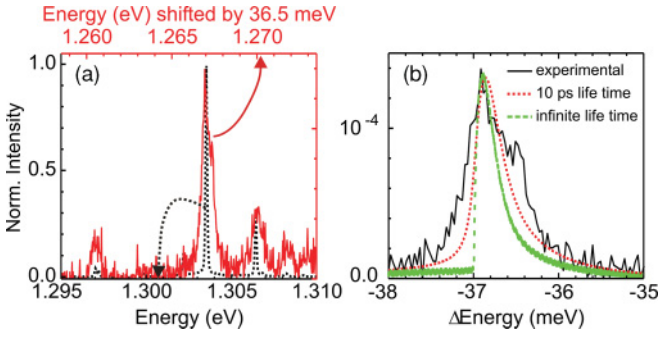

FIG. 3. (Color online) Optical-phonon replica of a single QD. (a) The black dotted curve shows three ZPL lines, each one having a replica, separated by 36.5 meV (red spectra, top energy scale). (b) Comparison of the LO line shape between experimentally measured (black) and calculated spectra with (red dotted curve) or without (green dashed curve) taking into account a finite lifetime of the phonon of 10 ps. A finite lifetime of the phonon provides a better description of the broad line shape of the LO phonon replica.

Next, we focus on the coupling strength of the exciton-LO phonon interaction. The coupling strength is usually described by the Huang-Rhys factor, given by the intensity ratio of the ZPL I_{ZPL} and the nth phonon replica I_n (at zero temperature) by $I_{\mathrm{n}}/I_{\mathrm{ZPL}} = S^n e^{-S}/n!$.[36,37] In Fig. 3 the intensity is normalized with respect to the ZPL. Both emission lines are located outside the cavity resonance in the stop band, so their intensities can be compared. The intensity of the LO phonon replica is about four orders of magnitude lower than the ZPL intensity, resulting in a Huang-Rhys factor of $S \approx 10^{-4}$. This value is one order of magnitude less than for GaAs bulk phonons,[38] indicating a reduced phonon coupling in our electrically pumped single QD. We additionally derived the Huang-Rhys factor from the calculated spectral density (Fig. 2).[37] Our calculations yield factors of $S \approx 10^{-4}$, confirming the experimental result.

The line shape of the phonon replicas enables us to access the coupling mechanism between the exciton and the LO phonon: The recombination of an electron-hole pair in a QD has a discrete energy and the linewidth of the ZPL is only limited by the lifetime of the exciton to a few μeV.[39] Therefore, any broadening of the luminescence upon generation of an LO phonon is due to the intrinsic phonon properties or coupling of the phonons to other modes. Figure 3 shows the LO phonon replica at larger spectral resolution. The resulting full width at half maximum of 700 μeV is well above the spectral resolution and about one hundred times larger than for the ZPL. Hence, LO phonons of varying energies are generated during the recombination processes in the same single QD. Also, the line shape is again slightly asymmetric, showing a faster decay on the low-energy side than on the high-energy side. This specific line shape is consistent with a broadening mechanism that results from a realistic wave-number-dependent LO phonon dispersion $\omega_{\mathrm{LO}}(q)$ beyond the Einstein model $\omega_{\mathrm{LO}} = \mathrm{const}$: In such a dispersion relation, a higher energy corresponds to a smaller momentum. Since the electron-phonon coupling favors low-momentum phonons, the generation of higher-energy phonons has a larger probability than that of lower-energy phonons, and thus yields an asymmetry of the line shape.

For a quantitative understanding of this coupling mechanism, we compare the experimental results with a model (Fig. 3), where LO phonon assisted luminescence spectra are calculated using the independent boson model and approximating the real optical-phonon dispersion by a cosine. This approximation agrees very well with the experimentally observed dispersion.[31] For the coupling matrix elements, we again compared Gaussian wave functions and eight-band $k\cdot p$ wave functions, respectively. In contrast to the acoustic phonon coupling, the influence of different wave functions is less pronounced. In Fig. 2 it can be seen that the LO phonon part of the spectral density shows a much faster decay than the acoustic phonon part. Hence the LO phonon replicas for Gaussian and eight-band $k\cdot p$ wave functions differ only slightly. For a complete description of the LO phonon-scattering process, we also included a finite lifetime of 10 ps (Refs. 40 and 41) of the LO phonons. The resulting LO replica in Fig. 3(b) reproduces very well the measured line shape, whereas a line shape with neglected phonon lifetime is too narrow. A perfect fit to the experimental data results in a phonon lifetime of 5 ps.

Additional phonon replica broadening, due to the influence of excited and wetting layer states, was predicted for the more enhanced electron-phonon coupling in CdSe systems.[25] We could not observe a significant influence in the GaAs material system in our calculations.

In conclusion, we studied the acoustic and optical phonon scattering on the most fundamental level, at which a single photon and a phonon are generated by the recombination of a single exciton in a single electrically driven InGaAs/GaAs QD. By comparing experimental and calculated spectra, we conclude that (i) GaAs bulk material phonon modes represent the dominant broadening mechanism; (ii) localized InAs-type phonons are not observed; (iii) a large LO-replica broadening of $\approx$700 μeV is induced by interaction with large wave-number phonons, having a finite lifetime; (iv) $k\cdot p$ wave functions are essential for the description of the excitons; and (v) the independent boson model using these wave functions provides the proper wave-vector dependence for a quantitative understanding of the experimental results.

We acknowledge fruitful discussions with A. Baumgartner and funding by the SFB 787 of the Deutsche Forschungsgemeinschaft (DFG).

*erik@sol.physik.tu-berlin.de

[1] D. Bimberg, M. Grundmann, and N. N. Ledentsov, *Quantum Dot Heterostructures* (Wiley, Chichester, 1998).
[2] P. Michler, A. Kiraz, C. Becher, W. V. Schoenfeld, P. M. Petroff, L. Zhang, E. Hu, and A. Imamoglu, Science **290**, 2282 (2000).
[3] A. J. Shields, Nat. Photonics **1**, 215 (2007).
[4] D. Bimberg *et al.*, IEEE Photon. J. **1**, 58 (2009).
[5] N. Akopian, N. H. Lindner, E. Poem, Y. Berlatzky, J. Avron, D. Gershoni, B. D. Gerardot, and P. M. Petroff, Phys. Rev. Lett. **96**, 130501 (2006).
[6] R. M. Stevenson, R. J. Young, P. Atkinson, K. Cooper, D. A. Ritchie, and A. J. Shields, Nature (London) **439**, 179 (2006).
[7] A. Schliwa, M. Winkelnkemper, A. Lochmann, E. Stock, and D. Bimberg, Phys. Rev. B **80**, 161307(R) (2009).
[8] C. Kindel, S. Kako, T. Kawano, H. Oishi, Y. Arakawa, G. Hönig, M. Winkelnkemper, A. Schliwa, A. Hoffmann, and D. Bimberg, Phys. Rev. B **81**, 241309(R) (2010).
[9] C. L. Salter, R. M. Stevenson, I. Farrer, C. A. Nicoll, D. A. Ritchie, and A. J. Shields, Nature (London) **465**, 594 (2010).
[10] N. Kirstaedter *et al.*, Electron. Lett. **30**, 1416 (1994).
[11] A. Marent, T. Nowozin, J. Gelze, F. Luckert, and D. Bimberg, Appl. Phys. Lett. **95**, 242114 (2009).
[12] H. J. Kimble, M. Dagenais, and L. Mandel, Phys. Rev. Lett. **39**, 691 (1977).
[13] B. Krummheuer, V. M. Axt, and T. Kuhn, Phys. Rev. B **65**, 195313 (2002).
[14] J. Forstner, C. Weber, J. Danckwerts, and A. Knorr, Phys. Rev. Lett. **91**, 127401 (2003).
[15] N. Gisin, G. Ribordy, W. Tittel, and H. Zbinden, Rev. Mod. Phys. **74**, 145 (2002).
[16] U. Hohenester, G. Pfanner, and M. Seliger, Phys. Rev. Lett. **99**, 047402 (2007).
[17] A. Carmele, F. Milde, M.-R. Dachner, M. B. Harouni, R. Roknizadeh, M. Richter, and A. Knorr, Phys. Rev. B **81**, 195319 (2010).
[18] J. P. Reithmaier, G. Sek, A. Loffler, C. Hofmann, S. Kuhn, S. Reitzenstein, L. V. Keldysh, V. D. Kulakovskii, T. L. Reinecke, and A. Forchel, Nature (London) **432**, 197 (2004).
[19] F. P. Laussy, E. del Valle, and C. Tejedor, Phys. Rev. Lett. **101**, 083601 (2008).
[20] G. Tarel and V. Savona, Phys. Rev. B **81**, 075305 (2010).
[21] R. Heitz, I. Mukhametzhanov, O. Stier, A. Madhukar, and D. Bimberg, Phys. Rev. Lett. **83**, 4654 (1999).
[22] A. V. Uskov, A. P. Jauho, B. Tromborg, J. Mork, and R. Lang, Phys. Rev. Lett. **85**, 1516 (2000).
[23] E. A. Muljarov and R. Zimmermann, Phys. Rev. Lett. **96**, 019703 (2006).
[24] A. V. Uskov, A. P. Jauho, B. Tromborg, J. Mork, and R. Lang, Phys. Rev. Lett. **96**, 019704 (2006).
[25] E. A. Muljarov and R. Zimmermann, Phys. Rev. Lett. **98**, 187401 (2007).
[26] R. Z. E. A. Muljarov, Phys. Status Solidi **245**, 1106 (2008).
[27] A. Carmele, M. Richter, W. W. Chow, and A. Knorr, Phys. Rev. Lett. **104**, 156801 (2010).
[28] A. Lochmann, E. Stock, J. A. Tofflinger, W. Unrau, A. Toropov, A. Bakarov, V. Haisler, and D. Bimberg, Electron. Lett. **45**, 566 (2009).
[29] R. Zimmermann and E. Runge, in *Proceedings of the 26th ICPS Edinburgh*, edited by J. H. Davies (IOP Publishing, Bristol, UK, 2002), Vol. 171, paper M 3.1.
[30] J. Forstner, C. Weber, J. Danckwerts, and A. Knorr, Phys. Status Solidi B **238**, 419 (2003).
[31] *Landolt-Börnstein—Semiconductors: Intrinsic Properties of Group IV Elements and II-V, II-VI and I-VII Compounds* (Springer, Berlin, 1987), Vol. III/22a.
[32] M. R. Dachner *et al.*, Phys. Status Solidi B **247**, 809 (2010).
[33] A. Wojs, P. Hawrylak, S. Fafard, and L. Jacak, Phys. Rev. B **54**, 5604 (1996).
[34] A. Schliwa, M. Winkelnkemper, and D. Bimberg, Phys. Rev. B **76**, 205324 (2007).
[35] R. Heitz *et al.*, Appl. Phys. Lett. **68**, 361 (1996).
[36] K. Huang and A. Rhys, Proc. R. Soc. A **204**, 406 (1950).
[37] V. May and O. Kühn, *Charge and Energy Transfer Dynamics in Molecular Systems* (Wiley-VCH Verlag, Berlin, 2000).
[38] S. Nomura and T. Kobayashi, Phys. Rev. B **45**, 1305 (1992).
[39] P. Borri, W. Langbein, S. Schneider, U. Woggon, R. L. Sellin, D. Ouyang, and D. Bimberg, Phys. Rev. Lett. **87**, 157401 (2001).
[40] S. Rudin, T. L. Reinecke, and M. Bayer, Phys. Rev. B **74**, 161305(R) (2006).
[41] A. R. Bhatt, K. W. Kim, and M. A. Stroscio, J. Appl. Phys. **76**, 3905 (1994).